ELSEVIER

Journal of Magnetism and Magnetic Materials 221 (2000) 57–62

Journal of magnetism and magnetic materials

www.elsevier.com/locate/jmmm

Low field magnetoresistance effects in fine particles of $La_{0.67}Ca_{0.33}MnO_3$ perovskites

J. Rivas[a,*], L.E. Hueso[a], A. Fondado[a], F. Rivadulla[b], M.A. López-Quintela[b]

[a]*Departamento de Física Aplicada, Universidad de Santiago de Compostela, E-15706 Santiago de Compostela, Spain*
[b]*Departamento de Química-Física, Universidad de Santiago de Compostela, E-15706 Santiago de Compostela, Spain*

Abstract

In this work magnetic and magnetotransport experimental data in well-characterized small particles of $La_{0.67}Ca_{0.33}MnO_3$ are presented. Grain size reduction leads to a larger resistivity and a decrease in metal–insulator transition temperature. Intrinsic colossal magnetoresistance (CMR) is destroyed while intergranular one is promoted to larger values. This low field MR can be explained taking into account magnetization data through spin-polarized tunneling model, which ensures an acceptable first-order fit between both magnitudes. Finally, low-temperature resistivity upturn present in small particle size samples can be understood in terms of an electrostatic barrier between grains.

Keywords: Magnetoresistance; Perovskites; Manganites; Grain boundaries; Sol–gel method

1. Introduction

Manganese mixed valence perovskites of the type $A_{1-x}B_xMnO_3$ (where A is a trivalent rare earth and B is a divalent element) have been the subject of intense research due to the huge values of magnetoresistance around the ferromagnetic transition temperature (T_C), the so-called Colossal Magnetoresistance (CMR) (see for a review Ref. [1]). Although no definitive theory has been presented at the moment, an attempt has been made to explain this intrinsic effect in terms of a mixture of double-exchange ferromagnetism between Mn^{3+} and Mn^{4+} ions and a strong spin–lattice interaction [2], which promotes the presence of magnetic polarons in the paramagnetic phase [3]. These polarons tend to collapse under the influence of a magnetic field and hence, electrical conductivity increases.

In polycrystalline samples, great values of low field magnetoresistance (LFMR) have been observed at temperatures well below T_C [4,5]. This extrinsic effect, that is absent in single crystals, seems to be related with transport across grain boundaries [5,6]. At the same time, other polycrystalline ferromagnetic materials show the same response to low magnetic fields (e.g. CrO_2, Fe_3O_4, Sr_2FeMoO_6) [7–9], much higher than in other known granular metals [10]. Several groups have constructed artificial devices and multilayers based on these compounds in order to improve MR, with great results, but specially on the low-temperature region [11–13].

In all these materials, half-metallic character (that is, 100% spin polarization of the carriers) is the clue of low field magnetoresistance values. In the particular case of mixed valence manganites,

* Corresponding author. Fax: + 34-981-520676.
E-mail address: farivas@uscmail.usc.es (J. Rivas).

0304-8853/00/$ - see front matter
PII: S0304-8853(00)00384-X

Mn^{3+} ($3d^4$) and Mn^{4+} ($3d^3$) are in an octahedral site symmetry; their electronic configuration being $t_{2g}^3 e_g^1$ for Mn^{3+} and t_{2g}^3 for Mn^{4+}. The e_g electrons are considered as mobile carriers interacting with the localized Mn^{4+} spins ($S = \frac{3}{2}$). The carrier hopping avoids the strong Hund's rule energy when the Mn spins are aligned ferromagnetically. Hund's rule energy is larger than the e_g bandwidth and the conduction electrons are completely spin polarized, as it was probed experimentally by Park et al. [14].

In this scenario, two possible theoretical mechanisms have been considered for the intergranular magnetoresistance. Intergranular spin-polarized tunneling assumes the presence of a magnetic barrier between grains with misalign spins that is reduced with the magnetic field favoring conductivity [5,15]. This model leads to an easy fitting equation for magnetoresistance:

$$\frac{\Delta\rho}{\rho_0} = -\left(\frac{JP}{4k_B T}\right)[m^2(H,T) - m^2(0,T)], \quad (1)$$

where J is the intergrain exchange constant, P the electron polarization (≈ 1 in manganites, as cited before), and m the magnetization normalized to the saturation value. Other suggestion is that low field MR is a consequence of spin-dependent scattering of polarized electrons across grain boundaries, which serve as pinning centers for the magnetic domain walls [16]. Although great numbers of experimental data are confusing, recent reports seem to confirm the spin polarized tunneling hypothesis [17,18].

In this work magnetic and transport data in well-characterized manganese perovskites nanoparticles are presented. By reducing grain size, the low field magnetoresistance effect is improved and can be related with magnetization data. At the same time, new and unexpected extrinsic results arise for smallest particles, that is, intrinsic CMR around metal–insulator transition temperature (T_{M-I}) is destroyed, and a strong localization effect appears at low temperatures.

2. Sample preparation and details

Ceramic samples of $La_{0.67}Ca_{0.33}MnO_3$ were prepared from high-purity oxides (CaO, La_2O_3, MnO and MnO_2, at least 99,995%) by conventional solid-state reaction, with a final sintering treatment of 100 h at 1300°C in a static air atmosphere. Nanometric particles were prepared by the sol–gel technique. We have employed an aqueous solution of $La(NO_3)_3 \cdot 6H_2O$, $Mn(NO_3)_2 \cdot 6H_2O$, $Ca(NO_3)_2 \cdot 4H_2O$ in stoichiometric proportions and urea as gelificant agent in a fixed concentration ($[urea]/[La^{3+}] + [Ca^{2+}] + [Mn^{2+}] = 10$). The geling agent and the molar relationship [urea]/[salts] was optimized to obtain homogeneous samples at lower temperatures, as it was described in detail by Vázquez-Vázquez et al. [19]. The solution is slowly evaporated until 137°C. When cooling, a gel is formed, and later, it is decomposed heating it at 250°C for 3 h, yielding the precursor to prepare the final samples. This precursor is annealed at different temperatures up to 1100°C for 6 h.

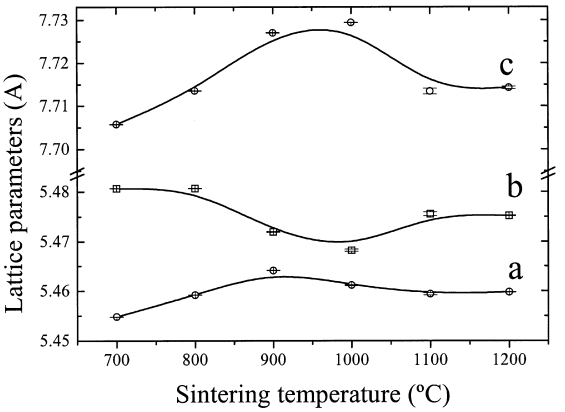

Fig. 1. Cell parameters for sol–gel samples annealed at different temperatures. Very small deviations are detected, indicating crystallization even for the lowest temperature studied.

X-ray powder patterns were collected at room temperature and fitted using the Rietveld method. In Fig. 1 we present lattice parameters obtained with this procedure. Very small variations are observed, because particles are completely crystallized for temperatures higher than 600°C. Particle sizes (D) were measured by means of scanning electron microscopy (SEM). In Fig. 2 (right), we plot the mean grain size change with different sintering temperatures. As it is observed, a gradual increase in size is obtained as temperature does. A deviation from the mean diameter smaller than 15% was

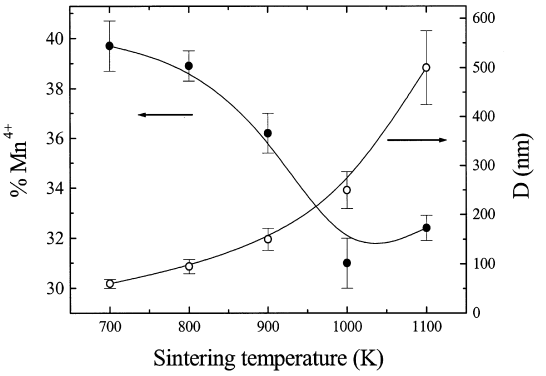

Fig. 2. Mn^{4+} percentage (left) and mean grain size (right) for sol–gel samples annealed at different temperatures. Lines are guides to the eye.

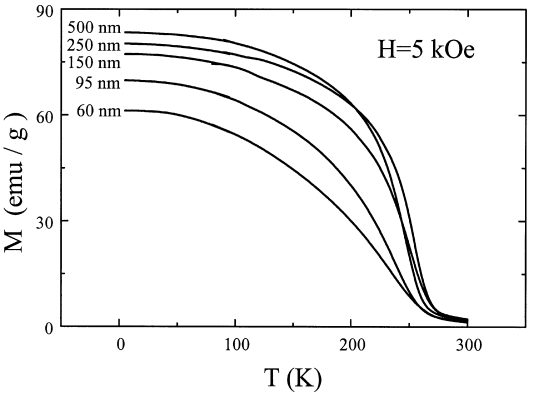

Fig. 3. Dependence of magnetization measured at 5 kOe with temperature for the samples with grain size ranging from 60 to 500 nm.

observed for all the samples. Moreover, the analysis revealed elongated rather than spherical particles. Merging temperature and sintering conditions we can modify grain size by more than three orders of magnitude. Mn^{4+} percentage was checked by yodometric analysis (see Fig. 2 left). High-temperature treated samples are nearly stoichiometric, but lower temperature ones present Mn^{4+} excess. Magnetization was measured using a SQUID magnetometer from 4 to 300 K. Resistivity measurements were made by the standard four-probe method at a constant current in the same temperature range and in field up to 50 kOe. Magnetoresistance is defined in usual way as $\%\ \mathrm{MR} = 100 \times (\rho(0) - \rho(H))/\rho(H = 0)$).

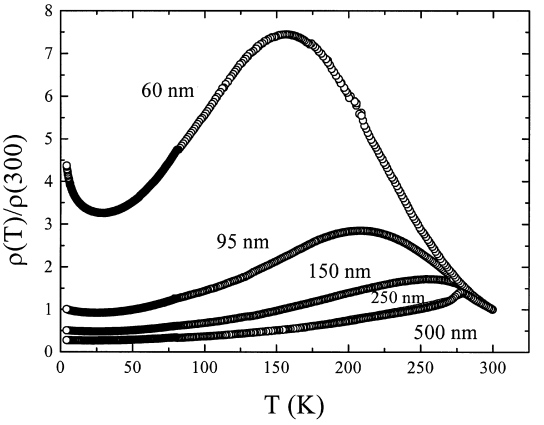

Fig. 4. Reduced resistivity versus temperature for nanocrystalline samples with grain size ranging from 60 to 500 nm.

3. Results and discussion

In Fig. 3 is shown magnetization measured at 5 kOe versus temperature for the sol–gel nanoparticles with grain size between 60 and 500 nm. In Fig. 4, we also plot the reduced electrical resistivity versus temperature for the same set of samples.

The behavior of the samples with larger grain size is very similar to the ceramic one (not plotted). They present the same metal–insulator transition temperature ($T_{M\text{–}I} \approx 265$ K), and it is also coincident with T_C. Moreover, low-temperature data are satisfactory, magnetization values are near to saturation magnetization, and the resistivity is quite low.

Nevertheless, reducing grain size, $T_{M\text{–}I}$ is translated to lower temperatures while ferromagnetic transition temperature remains unchanged, and low-temperature magnetization is far from saturation (see Figs. 3 and 4). This effect has been the center of controversy because of the great number of different experimental results and the different interpretations given [4,17,20–22]. Oxygen vacancies in low-temperature firing samples has been proposed as one of the reasons for the decrease in

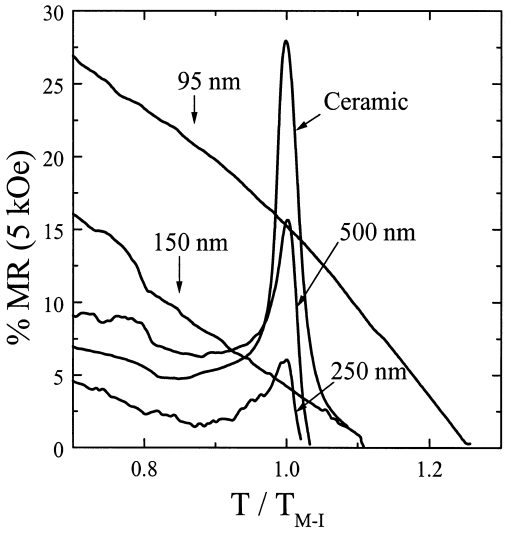

Fig. 5. Magnetoresistance at a constant field of 5 kOe (%MR) versus reduced temperature ($T/T_{M\text{-}I}$) for several particle size samples. The destruction of CMR peak is clearly observed for grain size smaller than 150 nm.

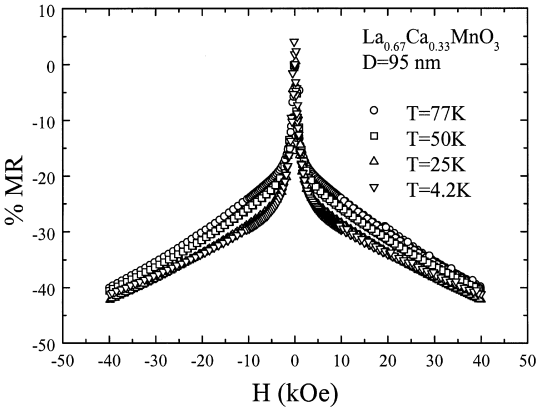

Fig. 6. Magnetoresistance versus magnetic field at several temperatures (sample with grain size of 95 nm). We can distinguish clearly between low field ($H < 5$ kOe) and high field responses ($H > 5$ kOe).

$T_{M\text{-}I}$ [22,23], but we have probed that this effect is not strong enough to account for the decrease obtained. Our hypothesis includes a mixture between oxygen vacancies and grain size dependence in $T_{M\text{-}I}$ behavior. The oxygen content (presented before in Fig. 2) should lead to a decrease in metal–insulator transition, as well as in ferromagnetic one, but not as large as presented here, if we compare it with $La_{1-x}Ca_xMnO_3$ phase diagram [24], where the complete Mn^{4+} range is studied. Thus, grain size contribution seems necessary to explain the results presented here.

Grain size reduction has another consequence in CMR effect. Progressive destruction of intrinsic colossal magnetoresistance is observed around metal–insulator transition (see Fig. 5). For sol–gel samples sintered at 900°C ($D \approx 150$ nm), colossal magnetoresistance completely disappears. Below the transition temperature, an increasing intergrain magnetoresistance response appears in every case, but it is the largest for smaller grain size samples. Intergrain MR remains measurable until $1.2T_{M\text{-}I}$ for the smallest grain sample. CMR tuning could be related with a transition from single domain to multidomain regime observed as grain size is increased, which promotes the presence of domain walls in the bigger particles [25]. The data presented here can be related to the theory developed by Zhang et al. [26]. This author relates the CMR peak in manganese perovskites to the presence of thermally activated magnetic domains. Although this kind of domains is different from static ones, the absence of domain walls could be related with the progressive destruction of the inherent mechanism that causes CMR.

Magnetoresistance behavior versus reduced temperature allows us to distinguish two separate groups of samples: samples treated at temperatures lower than 1000°C show the same steep slope in the evolution of MR versus T, that leads to a large value at low temperature. In contrast, high-temperature treated samples present the intrinsic CMR associated with metal–insulator transition and a small intergrain MR, with a less pronounced slope in the MR versus temperature curve.

Low-temperature MR shows a significant difference between low field and high field regimes (Fig. 6). Low field response occurs at $H < 5$ kOe and it is characterized by a sudden decrease in resistivity. Low field MR can achieve values as high as 33% for the samples studied. Its values are scalable with $1/D$ (see Fig. 7), so surface contribution is greater when the grain size is reduced, as expected before. However, high field MR is almost

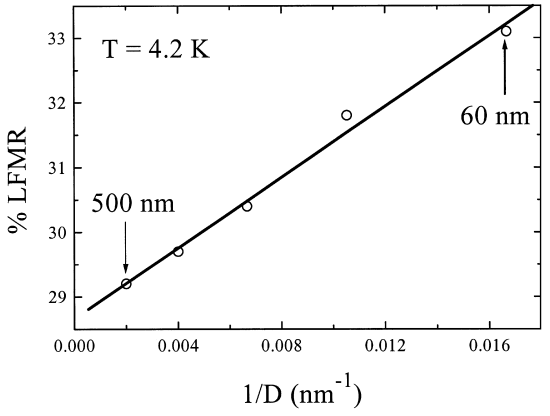

Fig. 7. Dependence of low field magnetoresistance (LFMR), that is, extrapolation of high field one to zero field, with inverse of grain size (surface/volume ratio) at 4.2 K.

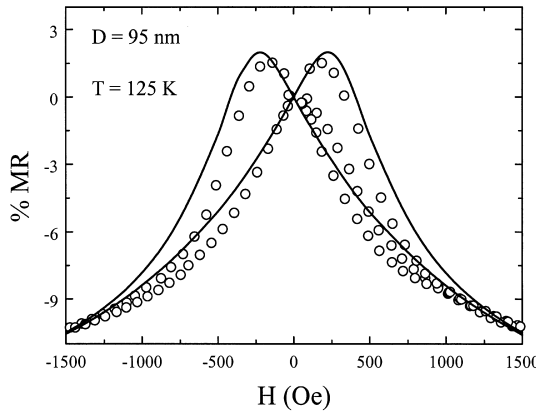

Fig. 8. Experimental (circles) and tunneling model fit (line) data of low field MR at 125 K for a sample with a grain size of 95 nm.

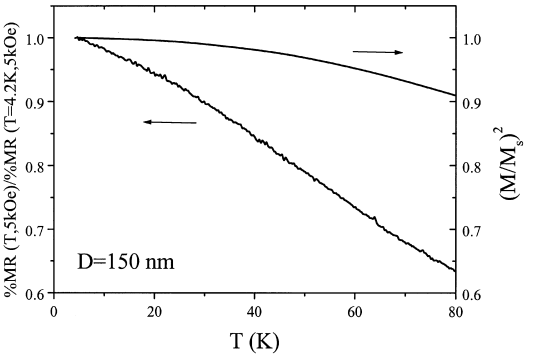

Fig. 9. Low field magnetoresistance (left axis) and square of magnetization (right axis) temperature dependence for a sol–gel sample with a mean particle size of 150 nm.

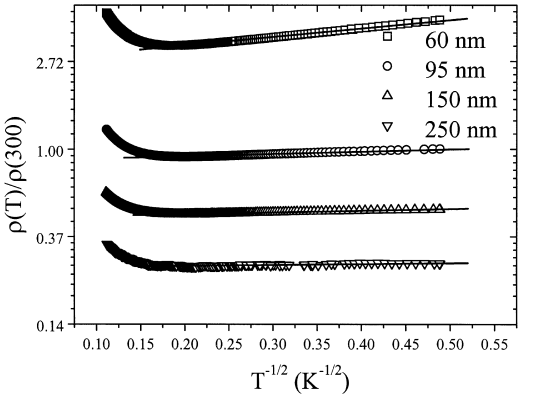

Fig. 10. Low-temperature resistivity fits $\rho(T) = A\exp(\sqrt{C/T})$. Slope of the fits is proportional to electrostatic energy barrier between grains.

linear with field, but the slope with field varies with temperature.

Spin-polarized tunneling model briefly presented before permit us to relate magnetoresistance and magnetization data at low temperatures, where this mechanism is predominant. Low field magnetoresistance versus magnetic field curves can be fitted to equation (1) taking J as a fitting factor (see Fig. 8) [22], but this factor has to be changed for a suitable relation in the whole range of temperature. The main reason is that LFMR decreases in temperature faster than the square of magnetization, as it is experimentally probed in Fig. 9. The reason for this fact is not clear today, and it is a lack of the model presented here but more theoretical work is in progress [18,27].

In the low-temperature range ($T < 35$ K), resistivity shows an upturn for smallest particle samples. This is another extrinsic effect that is not present in single crystals, but it is common in ceramic samples. Following theoretical results for granular metals [28], we have fitted $\ln \rho(T)$ versus $1/\sqrt{T}$ (Fig. 10). These fits assume the presence of an electrostatic barrier superimposed to the structural and magnetic one supposed in a single tunneling

model. This Coulomb energy obtained from fits is of the order of a few Kelvin, and increases as grain size decreases, making the localization effect more important. For ceramic and sol–gel samples sintered at high temperatures, its value is almost negligible. Its influence is responsible for the semiconductor behavior at low temperatures, but only in a restricted range of grain sizes.

In summary, we have presented new experimental results in small grain size $La_{0.67}Ca_{0.33}MnO_3$. Surface contribution seems to be responsible for a great variety of extrinsic effects. Great values of intergranular magnetoresistance arise in smaller grain size samples and, at the same time, intrinsic CMR around phase transition is destroyed. A model involving domain walls contribution and a spin-polarized tunneling below phase transition temperature could be the clue for this behavior. There are evidences that in small enough particles the observed electrical resistivity increase at very low temperatures could be ascribed to an electrostatic barrier present between grains.

Acknowledgements

L.E.H. thank M.E.C. for an F.P.I. grant, F.R. also acknowledges an F.P.U. grant from M.E.C. and U.S.C. This work has been financed by CICYT Spanish project MAT-98-0416.

References

[1] C.N.R. Rao, B. Raveau (Eds.), Colossal Magnetoresistance, Charge Ordering and Related Properties of Manganese Oxides, World Scientific, Singapore, 1998.
[2] H. Röder, Jun Zhang, A. Bishop, Phys. Rev. Lett. 76 (1996) 1356.
[3] J.M. De Teresa, M.R. Ibarra, P.A. Algarabel, C. Ritter, C. Marquina, J. Blasco, J. García, A. del Moral, Z. Arnold, Nature 386 (1997) 256.
[4] R.D. Sánchez, J. Rivas, C. Vázquez-Vázquez, M.A. López-Quintela, M.T. Causa, M. Tovar, S.B. Oseroff, Appl. Phys. Lett. 68 (1996) 134.
[5] H.Y. Hwang, S.-W. Cheong, N.P. Ong, B. Batlogg, Phys. Rev. Lett. 77 (1996) 2041.
[6] A. Urushibara, Y. Moritomo, T. Arima, A. Asamitsu, G. Kido, Y. Tokura, Phys. Rev. B 51 (1995) 14103.
[7] J.M.D. Coey, A.E. Berkowitz, Ll. Balcells, F.F. Putris, F.T. Parker, Appl. Phys. Lett. 72 (1998) 734.
[8] J.M.D. Coey, A.E. Berkowitz, Ll. Balcells, F.F. Putris, A. Barry, Phys. Rev. Lett. 80 (1998) 3815.
[9] K.-I. Kobayashi, T. Kimura, H. Sawada, K. Terakura, Y. Tokura, Nature 395 (1998) 677.
[10] A. Gerber, A. Milner, B. Groisman, M. Karpovsky, A. Gladkikh, A. Sulpice, Phys. Rev. B 55 (1997) 6446.
[11] Yu Lu, X.W. Li, G.Q. Gong, Gang Xiao, A. Gupta, P. Lecoeur, J.Z. Sun, Y.Y. Wang, V.P. Dravid, Phys. Rev. B 54 (1996) 8357.
[12] N.D. Mathur, G. Burnell, S.P. Isaac, T.J. Jackson, B.-S. Teo, J.L. MacManus-Driscoll, L.F. Cohen, J.E. Evetts, M.G. Blamire, Nature 387 (1997) 266.
[13] J.Z. Sun, D.W. Abraham, K. Roche, S.S.P. Parkin, Appl. Phys. Lett. 73 (1998) 1008.
[14] J.-H. Park, E. Vescovo, H.-J. Kim, C. Kwon, R. Ramesh, T. Venkatesan, Nature 392 (1998) 794.
[15] J.S. Helman, B. Abeles, Phys. Rev. Lett. 37 (1976) 1429.
[16] A. Gupta, G.Q. Gong, Gang Xiao, P.R. Duncombe, P. Lecouer, P. Troilloud, Y.Y. Wang, V.P. Dravid, J.Z. Sun, Phys. Rev. B 54 (1996) 15629.
[17] Ll. Balcells, J. Fontcuberta, B. Martínez, X. Obradors, Phys. Rev. B 58 (1998) 14 697.
[18] P. Raychaudhuri, K. Sheshadri, P. Taneja, S. Bandyopadhyay, P. Ayyub, A.K. Nigam, R. Pinto, S. Chaudhary, S.B. Roy, Phys. Rev. B 59 (1999) 13 919.
[19] C. Vázquez-Vázquez, M.C. Blanco, M.A. López-Quintela, R.D. Sánchez, J. Rivas, S.B. Oseroff, J. Mater. Chem. 8 (1998) 991.
[20] Ning Zhang, Weiping Ding, Wei Zhong, Dingyu Xing, Youwei Du, Phys. Rev. B 56 (1997) 8138.
[21] Lei Zheng, Kebin Li, Yuheng Zhang, Phys. Rev. B 58 (1998) 8631.
[22] L.E. Hueso, F. Rivadulla, R.D. Sánchez, D. Caeiro, C. Jardón, C. Vázquez-Vázquez, J. Rivas, M.A. López-Quintela, J. Magn. Magn. Mater. 189 (1998) 321.
[23] H.L. Ju, J. Gopalakrishnan, J.L. Peng, Qi Li, G.C. Xiong, T. Venkatesan, R.L. Greene, Phys. Rev. B 51 (1995) 6143.
[24] P. Schiffer, A.P. Ramirez, W. Bao, S.-W. Cheong, Phys. Rev. Lett. 75 (1995) 3336.
[25] L.E. Hueso, J. Rivas, F. Rivadulla, M.A. López-Quintela, J. Appl. Phys., in press.
[26] S. Zhang, Z. Yang, J. Appl. Phys. 79 (1996) 7398.
[27] S. Lee, H.Y. Hwang, B.I. Shraiman, W.D. Ratcliff II, S.-W. Cheong, Phys. Rev. Lett. 82 (1999) 4508.
[28] Ping Sheng, B. Abeles, Y. Arie, Phys. Rev. Lett. 31 (1973) 44.